Manner of Interaction of Heterogeneous Claudin Species Within and Between Tight Junction Strands

Mikio Furuse,* Hiroyuki Sasaki,‡§ and Shoichiro Tsukita*

*Department of Cell Biology, Faculty of Medicine, Kyoto University, Sakyo-ku, Kyoto 606-8501, Japan; ‡Laboratory of Cell Biology, KAN Research Institute Inc., Kyoto Research Park, Chudoji, Shimogyo-ku, Kyoto 600-8317, Japan; and §Department of Molecular Cell Biology, Institute of DNA Medicine, The Jikei University School of Medicine, Nishi-Shinbashi, Minato-ku, Tokyo 105-8461, Japan

Abstract. In tight junctions (TJs), TJ strands are associated laterally with those of adjacent cells to form paired strands to eliminate the extracellular space. Claudin-1 and -2, integral membrane proteins of TJs, reconstitute paired TJ strands when transfected into L fibroblasts. Claudins comprise a multigene family and more than two distinct claudins are coexpressed in single cells, raising the questions of whether heterogeneous claudins form heteromeric TJ strands and whether claudins interact between each of the paired strands in a heterophilic manner. To answer these questions, we cotransfected two of claudin-1, -2, and -3 into L cells, and detected their coconcentration at cell–cell borders as elaborate networks. Immunoreplica EM confirmed that distinct claudins were coincorporated into individual TJ strands. Next, two L transfectants singly expressing claudin-1, -2, or -3 were cocultured and we found that claudin-3 strands laterally associated with claudin-1 and -2 strands to form paired strands, whereas claudin-1 strands did not interact with claudin-2 strands. We concluded that distinct species of claudins can interact within and between TJ strands, except in some combinations. This mode of assembly of claudins could increase the diversity of the structure and functions of TJ strands.

Key words: tight junction • strand • claudin • cell adhesion • freeze-fracture

TIGHT junctions (TJs)[1] are the most apical component of the junctional complex in vertebrate epithelial and endothelial cells, and circumscribe individual cells as a belt-like structure. Ultrathin section and freeze-fracture EM have provided three-dimensional structural images of TJs (Farquhar and Palade, 1963; Staehelin, 1973, 1974). In the belt-like region of TJs, two apposing membranes lie close together, and within the lipid bilayer of each membrane, the so-called TJ strands, which are probably composed of linearly aggregated integral membrane proteins, form networks through their ramification. Each TJ strand laterally and tightly associates with that in the apposing membrane of adjacent cells to form a paired strand, where the intercellular distance becomes almost zero (see Fig. 1 A).

Address correspondence to Shoichiro Tsukita, M.D. and Ph.D., Department of Cell Biology, Faculty of Medicine, Kyoto University, Sakyo-ku, Kyoto 606-8501, Japan. Tel.: 81-75-753-4372. Fax: 81-75-753-4660. E-mail: htsukita@mfour.med.kyoto-u.ac.jp

1. *Abbreviations used in this paper:* E-face, extracellular face; pAb, polyclonal antibody; P-face, protoplasmic face; rTJ strand, reconstituted tight junction strand; TJ, tight junction.

Based on these structural, as well as functional, observations, dual functions have been proposed for TJs, both of which are crucial for the establishment of compositionally distinct compartments in multicellular systems (Schneeberger and Lynch, 1992; Gumbiner, 1993; Anderson and van Itallie, 1995; Yap et al., 1998). First, the formation of the paired TJ strands between adjacent cells seals the intercellular space as a permeability barrier to the diffusion of solutes through the paracellular pathway (barrier function of TJs). Morphological and physiological studies, however, predicted that TJs are not an absolute seal, but contain aqueous pores that fluctuate between open and closed states (Claude, 1978). Furthermore, the permeability, as well as ion selectivity, of TJs appeared to vary depending on epithelial cell type (for review see Powell, 1981). Second, the network of TJ strands within plasma membranes was regarded as the morphological counterpart for the barrier for the lateral diffusion of lipids and proteins between apical and basolateral membrane domains (fence function of TJs).

To date, two distinct types of integral membrane proteins, occludin and claudins, bearing four transmembrane domains have been identified as components of TJ strands (Furuse et al., 1993, 1998a; Ando-Akatsuka et al., 1996;

© The Rockefeller University Press, 0021-9525/99/11/891/13 $5.00

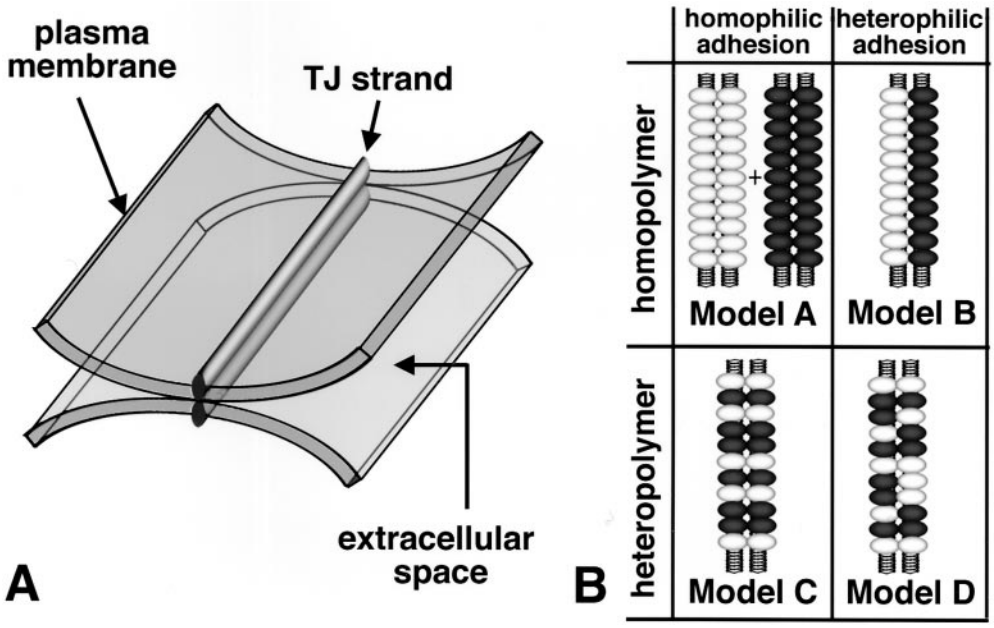

Figure 1. TJ strands and claudins. A, Schematic drawing of the TJ. At TJs, two apposing membranes lie close together, and TJ strands run within the lipid bilayer of each membrane. TJ strands in apposing membranes laterally associate to form paired strands, where the extracellular space is completely eliminated. B, Possible models of the arrangements of two distinct species of claudins (white and black spheroids) in each paired TJ strand. When each TJ strand is composed of a single species of claudin (homopolymer), two types of paired strands are formed by homophilic lateral association (homophilic adhesion; Model A) or heterophilic lateral association (heterophilic adhesion; Model B) of each TJ strand. When each TJ strand is a heteropolymer of two distinct species of claudins (heteropolymer), paired strands are formed by homophilic interaction (Model C) or heterophilic adhesion (Model D) of each claudin molecule.

Tsukita and Furuse, 1999). Recently, JAM, a member of the immunoglobulin superfamily, was also reported to be localized at TJs, but its involvement in the formation of TJ strands, per se, still remains unclear (Martin-Padura et al., 1998). Occludin, with a molecular mass of ~65 kD, was shown to be exclusively localized at TJ strands in various types of epithelial cells (Fujimoto 1995; Saitou et al., 1997) and to be involved not only in the barrier, but also in the fence functions of TJs (Balda et al., 1996; McCarthy et al., 1996; Chen et al., 1997; Wong and Gumbiner, 1997). However, occludin was undetectable in most endothelial cells of mammalian nonneuronal tissues and in Sertoli cells of the guinea pig/human testis, where TJs were observed (Hirase et al., 1997; Saitou et al., 1997; Moroi et al., 1998). Overexpression of mutant occludin resulted in changes in the distribution of occludin without affecting the structure or distribution of TJ strands (Balda et al., 1996). Furthermore, when occludin-deficient embryonic stem cells were established and differentiated into epithelium-like cells (visceral endoderm cells), well-developed networks of TJ strands were still formed between adjacent cells (Saitou et al., 1998). Considering that isoforms of occludin have not been found, these findings indicated that TJ strands can be formed without occludin.

Claudin-1 and -2 with molecular masses of ~23 kD were identified from the isolated junctional fraction from the liver as proteins that were copartitioned with occludin during sonication and density gradient centrifugation of the TJ-enriched fraction (Furuse et al., 1998a). These molecules showed no sequence similarity to occludin. Claudins comprise a multigene family, and to date 15 species of claudins have been identified (Furuse et al., 1998a; Morita et al., 1999a; Tsukita and Furuse, 1999). When claudins were introduced into mouse L fibroblasts, they were concentrated at cell–cell contact planes as an elaborate network, where well-developed networks of TJ strand-like structures were reconstituted (in this study, we tentatively call these reconstituted TJ strand-like structures in L cells rTJ strands). On the other hand, introduction of occludin induced only a small number of short TJ strand-like structures (Furuse et al., 1998b). When claudin and occludin were cotransfected into L cells, occludin appeared to be integrated into claudin-based rTJ strands.

These findings suggested that claudins are polymerized linearly within plasma membranes to constitute the backbone of TJ strands, and that occludin is copolymerized into these claudin-based strands. It is interesting to speculate that the existence of multiple claudin species can explain the diversity of the barrier function of TJs. To evaluate this speculation, however, it is necessary to understand in what manner multiple claudin species are incorporated into TJ strands. Northern blotting showed that the tissue distribution pattern varied significantly, depending on claudin species, and that many tissues expressed multiple claudin species (Furuse et al., 1998a; Morita et al., 1999a). Furthermore, immunofluorescence microscopy revealed that epithelial cells in distal tubules of the kidney expressed at least claudin-4 and -8, indicating that single cells coexpressed more than two species of claudins to constitute TJs. These observations have raised questions regarding whether in TJs in situ multiple distinct species of claudins are copolymerized linearly to form TJ strands as heteropolymers (Fig. 1 B), and whether claudins interact between each of the paired strands in a homophilic or heterophilic manner (Fig. 1 B). To address these questions, we established and examined L transfectants expressing claudin-1, -2, and -3 singly or in combination by immunofluorescence microscopy and conventional/immunolabeled

freeze-fracture EM. This study provided new insight into the structure and function of TJ strands.

Materials and Methods

Polyclonal and Monoclonal Antibody Production

Rabbit anti–mouse claudin-2 pAb and rabbit anti–mouse claudin-3 pAb were raised and characterized previously (Kubota et al., 1999; Morita et al., 1999a). Guinea pig anti–mouse claudin-1 pAb was raised against the synthetic polypeptides CPRKTTSYPTPRPYPKPTPSSGKD, which corresponds to the COOH-terminal cytoplasmic domains of mouse claudin-1 (amino acid 186–209). These pAbs were affinity-purified on nitrocellulose membranes with GST fusion proteins with the COOH-terminal cytoplasmic domain of respective claudins. GST fusion proteins were expressed in *Escherichia coli* (strain DH5α) and purified with the glutathione-Sepharose 4B beads (Amersham Pharmacia Biotech).

Rat anti–mouse claudin-1 mAb and rat anti–mouse claudin-2 mAb were produced as described previously (Itoh et al., 1991). Wistar rats were immunized with GST fusion proteins with the COOH-terminal cytoplasmic domain of respective claudins, and the lymphocytes were fused with P3 myeloma cells to obtain hybridoma cells. Fusion plates were screened by immunofluorescence staining of L transfectants expressing claudin-1 or -2 or by immunoblotting of GST fusion proteins. Mouse anti-FLAG mAb (M2) was purchased from Eastman Kodak Co.

Expression Vectors

To construct plasmids for the expression of GST/claudin-1 and GST/claudin-2 fusion proteins in *E. coli*, cDNAs encoding the COOH-terminal cytoplasmic region of claudin-1 (amino acid 188–211) and that of claudin-2 (amino acid 189–230) were amplified by PCR. Each cDNA fragment was subcloned into pGEX4T-1 (Amersham Pharmacia Biotech) to produce pGEX-IN (GST/claudin-1) and pGEX-IU (GST/claudin-2). The plasmid for the expression of GST/claudin-3 was constructed as described previously (Morita et al., 1999a).

The mammalian expression vectors for claudin-1, -2, and -3 were constructed as follows. The cDNA fragment containing the whole open reading frame of claudin-1 or -2 was excised from pGTCL-1 or pGTCL-2 (Furuse et al., 1998b) by SacI or EcoRI digestion, respectively. Each DNA fragment was subcloned into pCAGGSneodelEcoRI (Niwa et al., 1991) to produce the expression vectors pCCL-1 (claudin-1) and pCCL-2 (claudin-2). Similarly the whole open reading frame of claudin-3 cDNA was subcloned into pCAGGSneodelEcoRI to construct the expression vector pCCL-3 (Morita et al., 1999a). To construct the expression vector for the claudin-1 mutant lacking its COOH-terminal cytoplasmic domain, the cDNA fragment of claudin-1 corresponding to amino acid 148–188 was obtained by PCR using primers GGCGACATTAGTGGCCACAGCATG (sense) and CGCGGATCCTTTCCGGGGACAGGAGCA (antisense), followed by EcoRI and BamHI digestion. The cDNA fragment of claudin-1 encoding amino acid 148–211 was removed from the plasmid pSKCL-1F, which contained FLAG-tagged claudin-1 cDNA (Furuse et al., 1998a), by EcoRI and BamHI digestion and was replaced by this PCR-amplified truncated cDNA fragment. Then the FLAG-tagged COOH-terminal cytoplasmic domain-deleted claudin-1 cDNA was subcloned into the expression vector pCAGGSneodelEcoRI to make pCCL-1ΔCF.

Transfection

To establish L transfectants singly expressing claudin-1, -2, or -3 (C1L, C2L, and C3L, respectively), mouse L cells cultured in 35-mm dishes were transfected with 1 μg of pCCL-1, pCCL-2, or pCCL-3 in 1 ml of Opti-MEM using lipofectamine plus (GIBCO BRL). After 14–16-d selection in DME containing 500 μg/ml of G418, resistant colonies were picked up. Isolated clones were screened by immunofluorescence microscopy. C1C2L cells coexpressing claudin-1 and -2 were established by transfection of C1L cells with a mixture of 1 μg of pCCL-2 and 0.1 μg of pPGK-puro, and then selected in DME containing 8 μg/ml of puromycin. Similarly, C1C3L and C2C3L cells were produced by transfecting C3L cells with pCCL-1 and pCCL-2, respectively, together with pGKpuro. C1FC2L cells coexpressing claudin-1 with a FLAG tag at its COOH terminus and claudin-2 were established by transfecting C1FL cells expressing FLAG-claudin-1 (Furuse et al., 1998b) with 1 μg of pCCL-2 and 0.1 μg of pSV2hph (Santerre et al., 1984), followed by selection in 200 μg/ml of hygromycin B. C1ΔCFL cells expressing COOH-terminal cytoplasmic domain-truncated claudin-1 with FLAG-tag was produced by transfecting L cells with pCCL-1ΔCF, followed by G418 selection. Several stable clones were isolated for each transfection experiment. Among these, clone 16 of C1L, clone 12 of C2L, clone 17 of C3L, clone 1 of C1C2L, clone 12 of C1C3L, clone 15 of C2C3L, clone 11 of C1FC2L, and clone 16 of C1ΔCFL were recloned and used for this study, since they expressed relatively large amounts of introduced proteins. Mouse L cells and transfectants were cultured in DME supplemented with 10% FCS.

SDS-PAGE and Immunoblotting

SDS-PAGE was performed according to the method of Laemmli (1970), and proteins were electrophoretically transferred from gels onto polyvinylene difluoride membranes. The membranes were soaked in 5% skimmed milk and incubated with the primary antibodies. After washing, the membranes were incubated with the second antibodies for rat, rabbit (Amersham Pharmacia Biotech), or guinea pig (Chemicon International, Inc.) IgG, followed by incubation with streptavidin-conjugated alkaline phosphatase (Amersham Pharmacia Biotech). Nitroblue tetrazolium and bromochloroindolyl phosphate were used as substrates to visualize the enzyme reaction.

Immunofluorescence Microscopy

L transfectants (1.5×10^6 cells) were plated on 60-mm culture dishes with coverslips. For coculture, 7.5×10^5 cells of each transfectant were mixed and plated. After a 48-h culture, cells on coverslips were fixed with 1% formaldehyde in PBS for 10 min at room temperature, washed with PBS, and treated with 0.2% Triton X-100 in PBS for 10 min. Cells were then washed with PBS, soaked in 1% BSA in PBS, and incubated with primary antibodies for 30 min in a moist chamber. After washing with PBS three times, cells were incubated with the fluorescently labeled second antibodies for 30 min. FITC-conjugated goat anti–rat IgG (BioSource International), Cy3-conjugated goat anti–rabbit IgG (Amersham Pharmacia Biotech), Cy3-conjugated goat anti–mouse IgG (Amersham Pharmacia Biotech), rhodamine-conjugated goat anti–guinea pig IgG, and FITC-conjugated goat anti–rabbit IgG (Chemicon International, Inc.) were used as secondary antibodies. Cells were washed three times with PBS and then mounted in 90% glycerol-PBS containing para-phenylenediamine and 1% *n*-propylgalate. Frozen sections of mouse liver were stained immunofluorescently, as described previously (Furuse et al., 1993). Specimens were observed using a fluorescence Zeiss Axiophot photomicroscope, and the images were recorded with a SensysTM cooled CCD camera system (Photometrics).

Freeze-fracture Electron Microscopy

For conventional freeze-fracture EM, L transfectants cultured on 60-mm dishes were fixed with 2% glutaraldehyde in 0.1 M sodium cacodylate buffer (pH 7.3) overnight at 4°C, washed with 0.1 M sodium cacodylate buffer three times, immersed in 30% glycerol in 0.1 M sodium cacodylate buffer for 2 h, and then frozen in liquid nitrogen. Frozen samples were fractured at −100°C and platinum-shadowed unidirectionally at an angle of 45° in Balzers Freeze Etching System (BAF060, BAL-TEC). Samples were then immersed in household bleach, the replicas floating off the samples were picked up on formvar-filmed grids and examined with a JEOL 1200 EX electron microscope at an acceleration voltage of 100 kV.

Immunoelectron microscopy for examining freeze-fracture replicas was performed as described by Fujimoto (1995). Mouse liver was cut into small pieces and quickly frozen in high pressure liquid nitrogen with an HPM010 high pressure freezing machine (BAL-TEC). L transfectants were fixed with 1% paraformaldehyde in 0.1 M phosphate buffer (pH 7.3) for 5 min at room temperature, washed three times in 0.1 M phosphate buffer, immersed in 30% glycerol in 0.1 M phosphate buffer for 3 h, and then frozen in liquid nitrogen. Frozen samples were then fractured and shadowed as described. Samples were immersed and stirred in lysis buffer containing 2.5% SDS, 10 mM Tris-HCl, and 0.6 M sucrose (pH 8.2) for 12 h at room temperature, then replicas floating off the samples were washed with PBS containing 5% BSA. The replicas were incubated with primary antibodies for 2 h, washed with PBS-BSA, incubated with colloidal gold-conjugated secondary antibodies, washed with PBS-BSA, and then picked up on formvar-filmed grids. Goat anti–rabbit IgG coupled with 5-nm gold, goat anti–mouse IgG coupled with 15-nm gold (Amersham Pharmacia Biotech), and goat anti–guinea pig IgG coupled with 15-nm gold (British BioCell International) were used as secondary antibodies.

Results

Characterization of Antibodies and L Transfectants Expressing Claudin-1, -2, or -3

We raised monoclonal and polyclonal antibodies against the COOH-terminal cytoplasmic domains of claudin-1, -2, and -3. Immunoblotting of GST fusion proteins with the COOH-terminal tails of claudin-1, -2, and -3 confirmed the specificity of these antibodies (Fig. 2 A). Then, cDNAs encoding claudin-1, -2, and -3 were transfected into L fibroblasts and stable transfectants were obtained (C1L, C2L, and C3L cells, respectively). When the total cell lysates of these transfectants were immunoblotted with anti-claudin-1, -2, and -3 pAbs, bands of respective claudins with the expected molecular masses were clearly detected (Fig. 2 B).

Previously, we obtained L transfectants stably expressing claudin-1 or -2 that were tagged with a FLAG sequence at their COOH termini (C1FL and C2FL cells, respectively) and found that introduced FLAG-claudin-1 and -2 were concentrated at cell–cell contact planes in an elaborate network pattern (Furuse et al., 1998b). Immunofluorescence microscopy of C1L, C2L, and C3L cells with anti-claudin-1, -2, or -3 antibodies revealed that introduced claudin-1, -2, and -3 without an epitope tag were also highly concentrated at cell–cell borders to form elaborate networks (Fig. 2 C). Similar to C1FL and C2FL cells, well-developed networks of rTJ strands/grooves were induced at these cell–cell contact planes of C1L, C2L, and C3L cells, as revealed by conventional freeze-fracture EM (see Fig. 5, g–i and Fig. 8, a and b). Judging from the morphological characteristics, as well as the size of the networks detected by immunofluorescence microscopy at cell–cell contact planes (Fig. 2 C, c, f, i, l, and o), each line in these networks can be regarded to represent individual rTJ strands. These immunofluorescence observations further

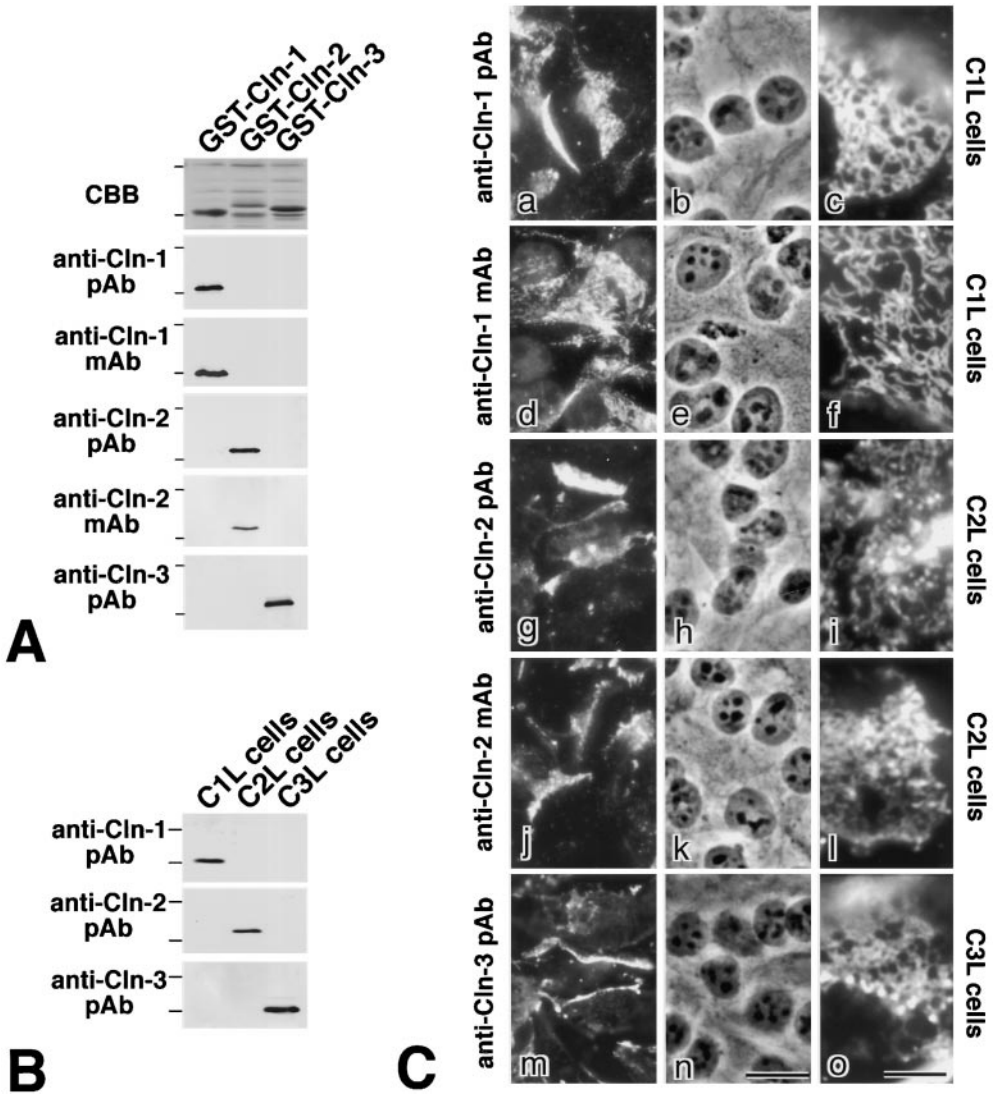

Figure 2. Anticlaudin antibodies and L transfectants expressing claudin-1, -2, or -3. A, GST fusion proteins with the COOH-terminal cytoplasmic domains of claudin-1 (GST-Cln-1), claudin-2 (GST-Cln-2), and claudin-3 (GST-Cln-3) were separated by SDS-PAGE (CBB), and immunoblotted with guinea pig anticlaudin-1 pAb (anti-Cln-1 pAb), rat anticlaudin-1 mAb (anti-Cln-1 mAb), rabbit anticlaudin-2 pAb (anti-Cln-2 pAb), rat anticlaudin-2 mAb (anti-Cln-2 mAb), and rabbit anticlaudin-3 pAb (anti-Cln-3 pAb). Each GST fusion protein was specifically detected by respective pAb or mAb. B, Total cell lysates of L transfectants expressing claudin-1 (C1L cells), claudin-2 (C2L cells), or claudin-3 (C3L cells) were separated by SDS-PAGE and immunoblotted with anticlaudin-1 pAb (anti-Cln-1 pAb), anti-claudin-2 pAb (anti-Cln-2 pAb), or anticlaudin-3 pAb (anti-Cln-3 pAb). The bands of respective claudins with expected molecular masses were specifically detected. Bars indicate molecular masses of 31 and 21 kD, respectively, from the top. C, C1L, C2L, and C3L cells were immunofluorescently stained with respective antibodies (a, d, g, j, and m). b, e, h, k, and n, Corresponding phase-contrast images. Expressed claudins were specifically found to be concentrated at cell–cell borders as planes. At higher magnification, claudins were seen to be distributed in an elaborate network pattern in these planes (c, f, i, l, and o). Bars: (a, b, d, e, g, h, j, k, m, and n) 10 μm; (c, f, i, l, and o) 3 μm.

confirmed the specificity of anticlaudin-1, -2, and -3 pAbs and mAbs used in this study.

TJ Strands as Heteropolymers of Distinct Species of Claudins

Northern blotting revealed that several distinct species of claudins are coexpressed in individual organs, such as the lung, liver, and kidney (Furuse et al., 1998a; Morita et al., 1999a). Since claudin-1, -2, and -3 appeared to be expressed in the liver, we first double stained frozen sections of the mouse liver with guinea pig anticlaudin-1 pAb/rabbit anticlaudin-2 pAb or guinea pig anticlaudin-1 pAb/rabbit anticlaudin-3 pAb. As shown in Fig. 3, a–d, claudin-1, -2, and -3 were colocalized at the junctional complex regions along bile canaliculi. These findings indicated that claudin-1, -2, and -3 were evenly mixed in these cells, at least at the level of immunofluorescence microscopy. Furthermore, the freeze-fracture replicas obtained from mouse liver were double labeled with anticlaudin-1 pAb and anticlaudin-3 pAb (Fig. 3 e). Although, with unknown reason, the labeling ability of guinea pig anticlaudin-1 pAb for freeze-fracture replicas was very low, the 15-nm and 5-nm gold particles representing the localization of claudin-1 and -3, respectively, appeared to be admixed along individual TJ strands. Therefore, at the level of TJ strands, it was likely that claudin-1, -2, and -3 were copolymerized into individual TJ strands as heteropolymers of claudins (see Fig. 1 B, Model C and D).

To evaluate this possibility, we used L transfectants as a model system. As shown previously (Furuse et al., 1998b) and in Fig. 2 C, claudin-1, -2, and -3 can form homopolymers in L transfectants. We then cotransfected claudin-1 and -2, claudin-1 and -3, or claudin-2 and -3, and obtained stable transfectants (C1C2L, C1C3L, or C2C3L cells, respectively; Fig. 4 A). When confluent cultures of C1C2L cells were double stained with anticlaudin-1 mAb and anticlaudin-2 pAb, both species of claudins showed the same concentration pattern at cell–cell contact planes (Fig. 4 B, a and b). Also, at higher magnification, almost identical network patterns of staining were observed at cell–cell contact planes by anticlaudin-1 mAb and anticlaudin-2 pAb (Fig. 4 B, g–i). Similarly, claudin-1 and -3, and claudin-2 and -3 were also colocalized in C1C3L and C2C3L cells, respectively (Fig. 4 B, c–f).

Next, we observed the morphology of rTJ strands in C1C2L, C1C3L, and C2C3L cells by conventional freeze-fracture EM. As previously shown in C1FL and C2FL cells (Furuse et al., 1998b), in glutaraldehyde-fixed C1L cells claudin-1–induced strands were largely associated with the protoplasmic (P) -face as mostly continuous structures with vacant grooves at the extracellular (E) -face (P-face–associated TJs; see Fig. 5 g), whereas in C2L cells claudin-2–induced strands were discontinuous at the P-face with

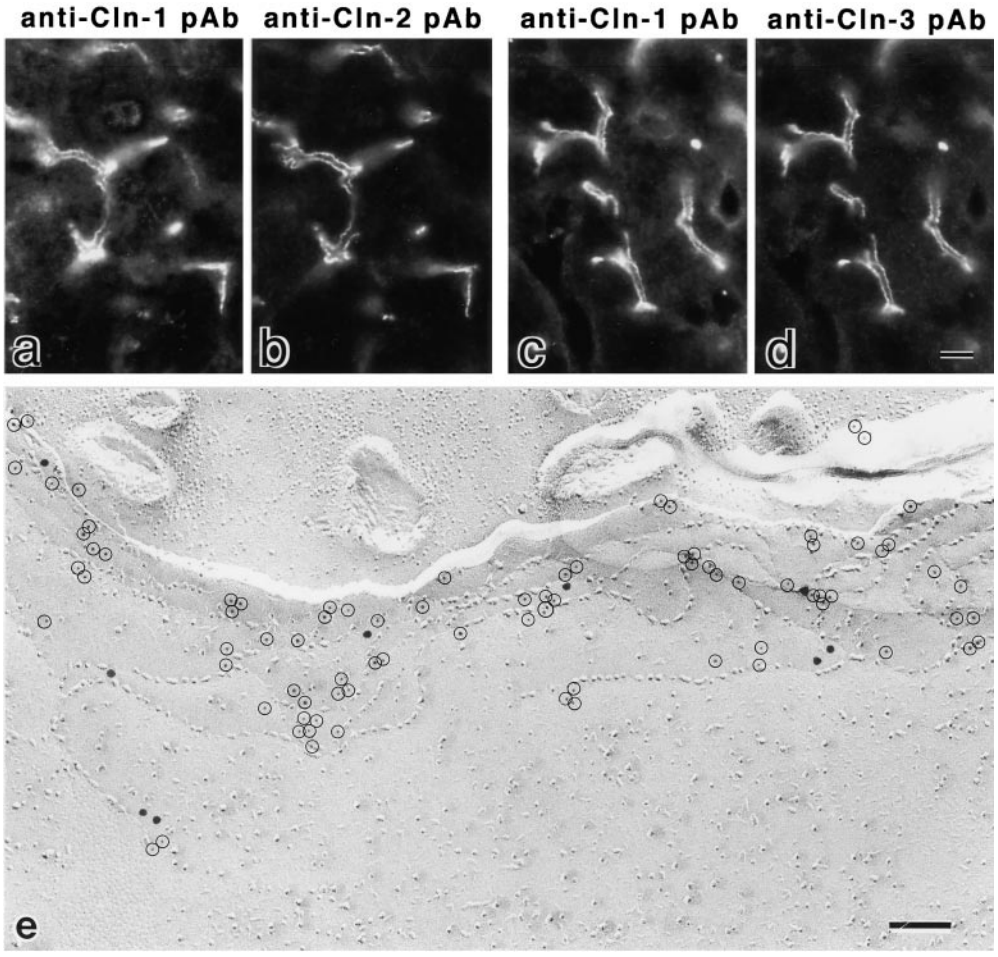

Figure 3. Codistribution of claudin-1, -2, and -3 in TJs of the mouse liver. a–d, Frozen sections of the liver were double stained with guinea pig anticlaudin-1 pAb (a)/rabbit anticlaudin-2 pAb (b) or guinea pig anticlaudin-1 pAb (c)/rabbit anticlaudin-3 pAb (d). Claudin-1, -2, and -3 were precisely colocalized at the junctional complex regions, although the expression levels of claudin-1 and -2 appeared to vary significantly, depending on the position of hepatocytes in lobules (data not shown). e, Freeze-fracture replicas of mouse liver were double labeled with anticlaudin-1 pAb (15-nm gold) and anticlaudin-3 pAb (5-nm gold). 5-nm gold particles were encircled. Although the labeling ability of anticlaudin-1 pAb was very low, these images suggested that claudin-1 and -3 were copolymerized into individual TJ strands in the liver. Bars: (a–d) 6 μm; (e) 100 nm.

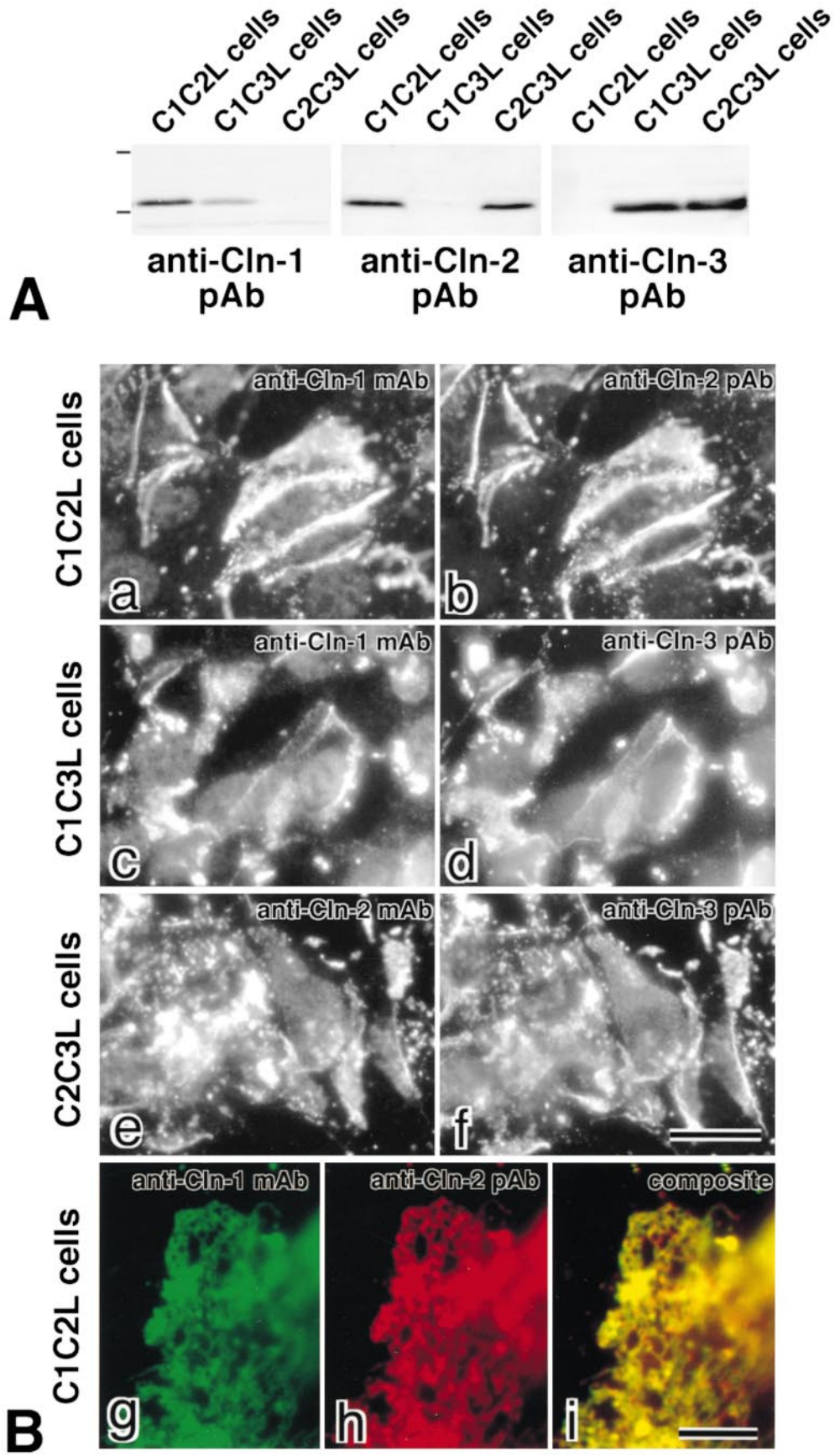

Figure 4. L transfectants co-expressing claudin-1 and -2 (C1C2L cells), claudin-1 and -3 (C1C3L cells), and claudin-2 and -3 (C2C3 cells). A, Total cell lysates of C1C2L, C1C3L, and C2C3L cells were immunoblotted with anticlaudin-1 pAb (anti-Cln-1 pAb), anticlaudin-2 pAb (anti-Cln-2 pAb), or anticlaudin-3 pAb (anti-Cln-3 pAb). Respective claudins with expected molecular masses were detected. Bars indicate molecular masses of 31 and 21 kD, respectively, from the top. B, Semiconfluent cultures of C1C2L, C1C3L, and C2C3L cells were double stained with anticlaudin-1 mAb (a)/anticlaudin-2 pAb (b), anticlaudin-1 mAb (c)/anticlaudin-3 pAb (d), and anticlaudin-2 mAb (e)/anticlaudin-3 pAb (f), respectively. Coexpressed claudins were precisely colocalized. At higher magnification of C1C2L cells, in the cell–cell contact planes, claudin-1 and -2 were precisely coconcentrated in an elaborate network (g–i), suggesting that claudin-1 and -2 were coincorporated into rTJ strands. Bars: (a–f) 10 μm; (g–i) 3 μm.

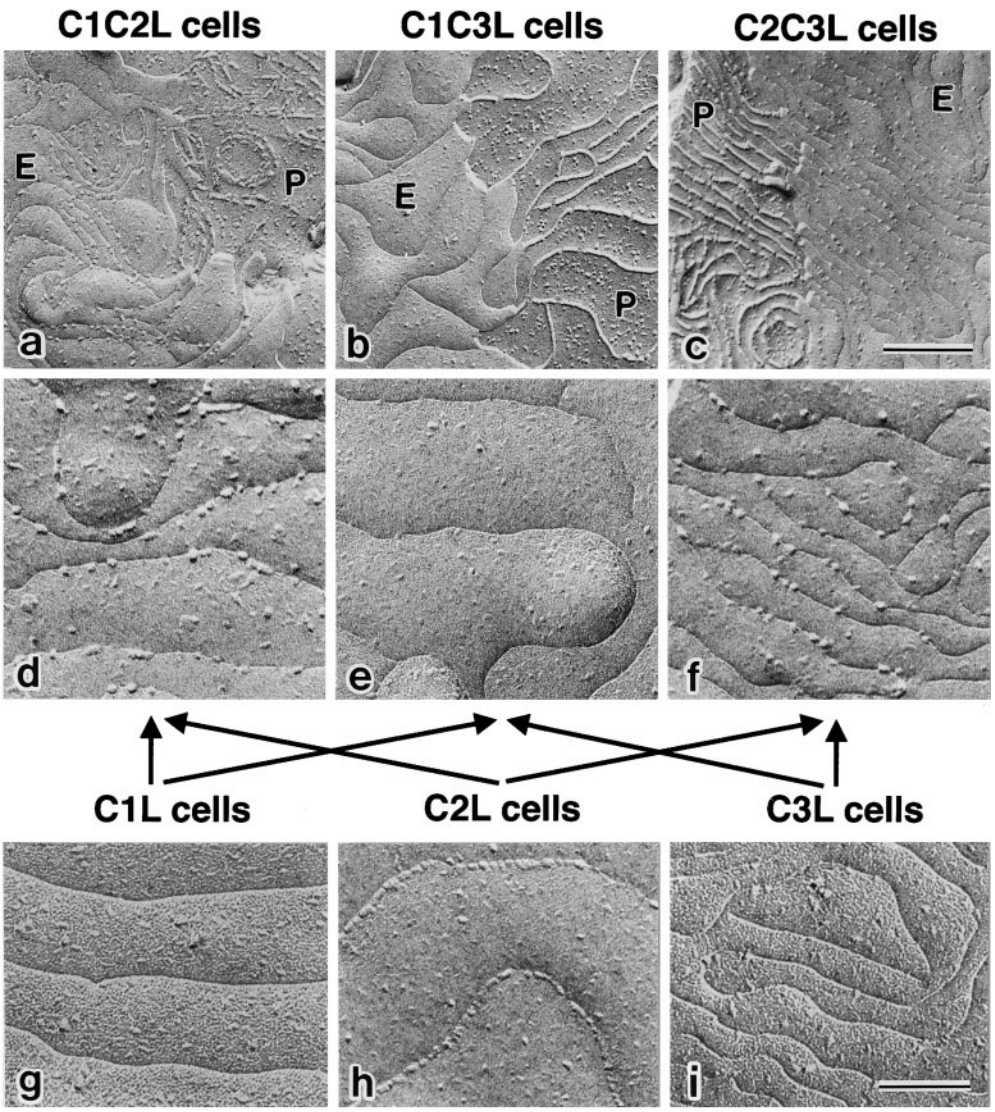

Figure 5. Freeze-fracture replica images of rTJ strands in C1C2L, C1C3L, and C2C3L cells. In the cell–cell contact planes of these cells, well-developed networks of rTJ strands were observed. As previously shown in C1FL and C2FL cells (Furuse et al., 1998b), in glutaraldehyde-fixed C1L cells, claudin-1–induced strands were largely associated with the P-face as mostly continuous structures (data not shown) with vacant grooves at the E-face (g; P-face–associated TJs), whereas in C2L cells, claudin-2–induced strands were discontinuous at the P-face (data not shown) with complementary grooves at the E-face that were occupied by chains of particles (h; see Fig. 8 a; E-face–associated TJs). Similar to C1L cells, P-face–associated TJs with vacant grooves on the E-face (i) were induced in C3L cells (see Fig. 8 b). C1C3L cells bore typical P-face–associated TJs (b), whereas C1C2L and C2C3L cells showed an intermediate morphology of rTJ strands/grooves between P- and E-face–associated TJs (a and c); the grooves at the E-face of C1C3L cells were completely vacant (e), whereas those in C1C2L and C2C3L cells were characterized by evenly scattered particles (d and f). Bars: (a–c) 200 nm; (d–i) 100 nm.

complementary grooves at the E-face that were occupied by chains of particles (E-face associated TJs; see Figs. 5 h and 8 a; Tsukita and Furuse, 1999). Similar to C1L cells, P-face–associated TJs were induced in C3L cells (see Figs. 5 i and 8 b). Interestingly, C1C3L cells bore typical P-face–associated TJs (Fig. 5 b), whereas C1C2L and C2C3L cells showed an intermediate morphology of rTJ strands/grooves between P- and E-face–associated TJs (Fig. 5, a and c); the grooves at E-face of C1C3L cells were completely vacant (Fig. 5 e), whereas those in C1C2L and C2C3L cells were characterized by evenly scattered particles (Fig. 5, d and f). These findings suggested that two distinct species of claudins were completely mixed up in individual rTJ strands in these L transfectants.

To confirm this speculation, the freeze-fracture replicas obtained from confluent C1C2L cells were double immunolabeled with guinea pig anticlaudin-1 pAb and rabbit anticlaudin-2 pAb. As shown in Fig. 6 a, the 15- and 5-nm gold particles representing the localization of claudin-1 and -2, respectively, appeared to be admixed along individual rTJ strands. Similar results were also obtained in C1C3L cells (Fig. 6 b). However, as described above, the labeling ability of anticlaudin-1 pAb for freeze-fracture replicas was fairly low (see Fig. 3 e). Therefore, we obtained L transfectants coexpressing claudin-2 and FLAG-tagged claudin-1 (C1FC2L cells), and the freeze-fracture replicas obtained from confluent C1FC2L cells were double labeled with anti-FLAG mAb (15-nm gold particles) and anticlaudin-2 pAb (5-nm gold particles; Fig. 6, c and d). In these images, numerous 15- and 5-nm gold particles appeared to distribute evenly and specifically along individual rTJ strands. Taken together with Fig. 5, we concluded that in the model system of L transfectants, distinct species of claudins can be copolymerized to form rTJ strands as heteropolymers (see Fig. 1 B, Model C or D).

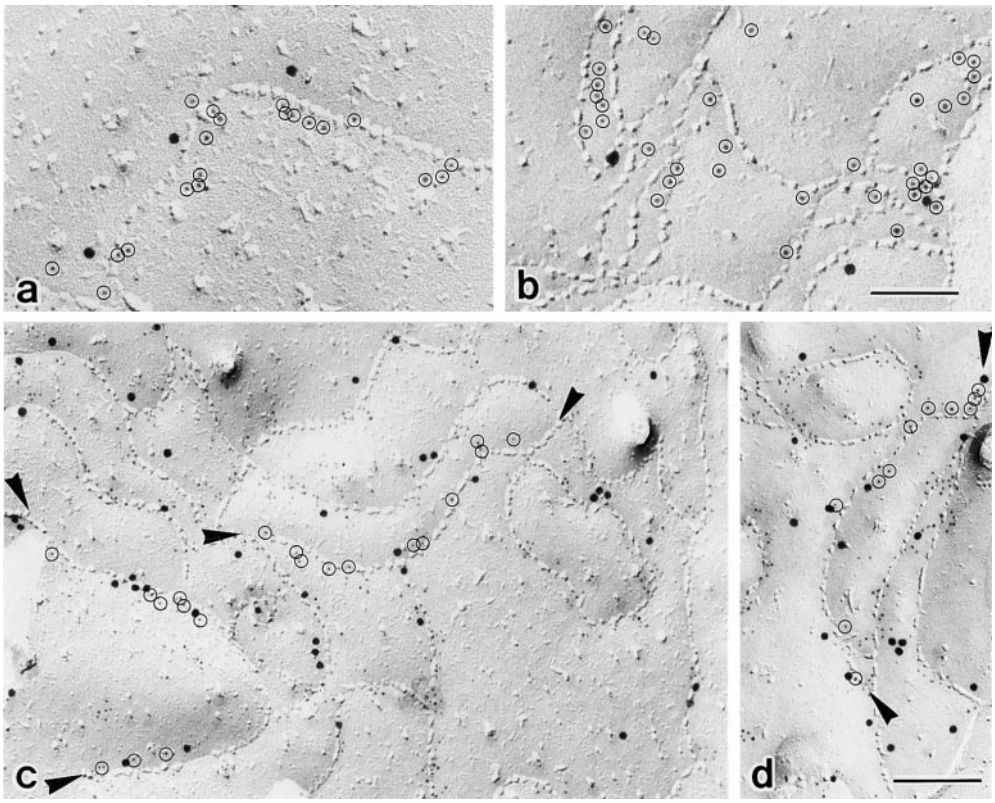

Figure 6. Immunoreplica EM of C1C2L and C1C3L cells. a and b, Freeze-fracture replicas of C1C2L and C1C3L cells were double labeled with guinea pig anticlaudin-1 pAb (15-nm gold)/rabbit anticlaudin-2 pAb (5-nm gold; a) and guinea pig anticlaudin-1 pAb (15-nm gold)/rabbit anticlaudin-3 pAb (5-nm gold; b), respectively. 5-nm gold particles were encircled. Although the labeling ability of anticlaudin-1 pAb was fairly low, the 15- and 5-nm gold particles appeared to be admixed along individual rTJ strands. c and d, Freeze-fracture replicas of C1FC2L cells were double labeled with mouse anti-FLAG mAb (15-nm gold) and rabbit anticlaudin-2 pAb (5-nm gold). 5-nm gold particles on selected rTJ strands (between two arrowheads) were encircled. Numerous 15- and 5-nm gold particles distribute evenly and specifically along individual rTJ strands. Bars: (a and b) 100 nm; (c and d) 150 nm.

Heterophilic Interaction of Distinct Species of Claudins between TJ Strands in Their Lateral Association

As described in Fig. 1 A, in TJs each TJ strand associates laterally with another TJ strand in the apposing membrane, which is responsible for intercellular adhesion at TJs. The next question was whether this lateral association, i.e., the cell adhesion at TJs, is attributable to homophilic or heterophilic interactions of the extracellular regions of claudins. Since paired rTJ strands were induced in C1L, C2L, and C3L cells, the homophilic interaction of claudins, as described in Model A (Fig. 1 B) can be expected in these cells. We next examined the possibility of the heterophilic interaction of claudins between homopolymers (Fig. 1 B, Model B) by coculturing pairs of C1L, C2L, and C3L cells.

As shown in Fig. 7 a–c, when C1L and C3L cells were cocultured and double stained with anticlaudin-1 mAb and anticlaudin-3 pAb, three types of cell–cell contact planes were distinguished in terms of immunofluorescence staining: the claudin-1–positive/claudin-3–negative planes, which would be formed between adjacent C1L cells; the claudin-1–negative/claudin-3–positive planes, which would be formed between adjacent C3L cells; and the claudin-1–positive/claudin-3–positive planes, which would be formed between adjacent C1L and C3L cells. At higher magnification, in the claudin-1–positive/claudin-3–positive planes, both claudin-1 and claudin-3 in C1L and C3L cells, respectively, were concentrated in an elaborate network pattern (Fig. 7, j and k), and their networks were mostly overlapped (Fig. 7 l). The same results were obtained in cocultures of C2L and C3L cells (Fig. 7, d–f and m–o). These findings indicated that claudin-3–based homopolymers (rTJ strands) can associate laterally with claudin-1– and claudin-2–based homopolymers through the heterophilic interactions of claudin-3 with claudin-1 and claudin-2, respectively. In contrast, when C1L and C2L cells were cocultured and double stained with anticlaudin-1 mAb and anticlaudin-2 pAb, the claudin-1–positive/claudin-2–positive planes were not formed (Fig. 7, g–i). Therefore, it was likely that, at least in L transfectants, claudin-1 cannot interact with claudin-2 in a heterophilic manner. In conclusion, in L transfectants, paired strands can be formed not only by homophilic interactions, but also by heterophilic interactions of claudins, except for some combinations of claudins.

To further confirm this conclusion, confluent cocultures of C2L and C3L cells were fixed with glutaraldehyde and examined by conventional freeze-fracture EM (Fig. 8). As described above, induced TJs in C2L and C3L cells were E- and P-face–associated, respectively, i.e., the fracture planes at C2L/C2L contact planes showed discontinuous strands on the P-face (P-C2L in Fig. 8 a) and grooves occupied with chains of particles on the E-face (E-C2L in Fig. 8 a), while the fracture planes at the C3L/C3L contact planes showed continuous strands on the P-face (P-C3L in Fig. 8 b) and vacant grooves on the E-face (E-C3L in Fig. 8 b). In the C2L/C3L coculture, in addition to these C2L/C2L and C3L/C3L fracture planes, fracture planes, which

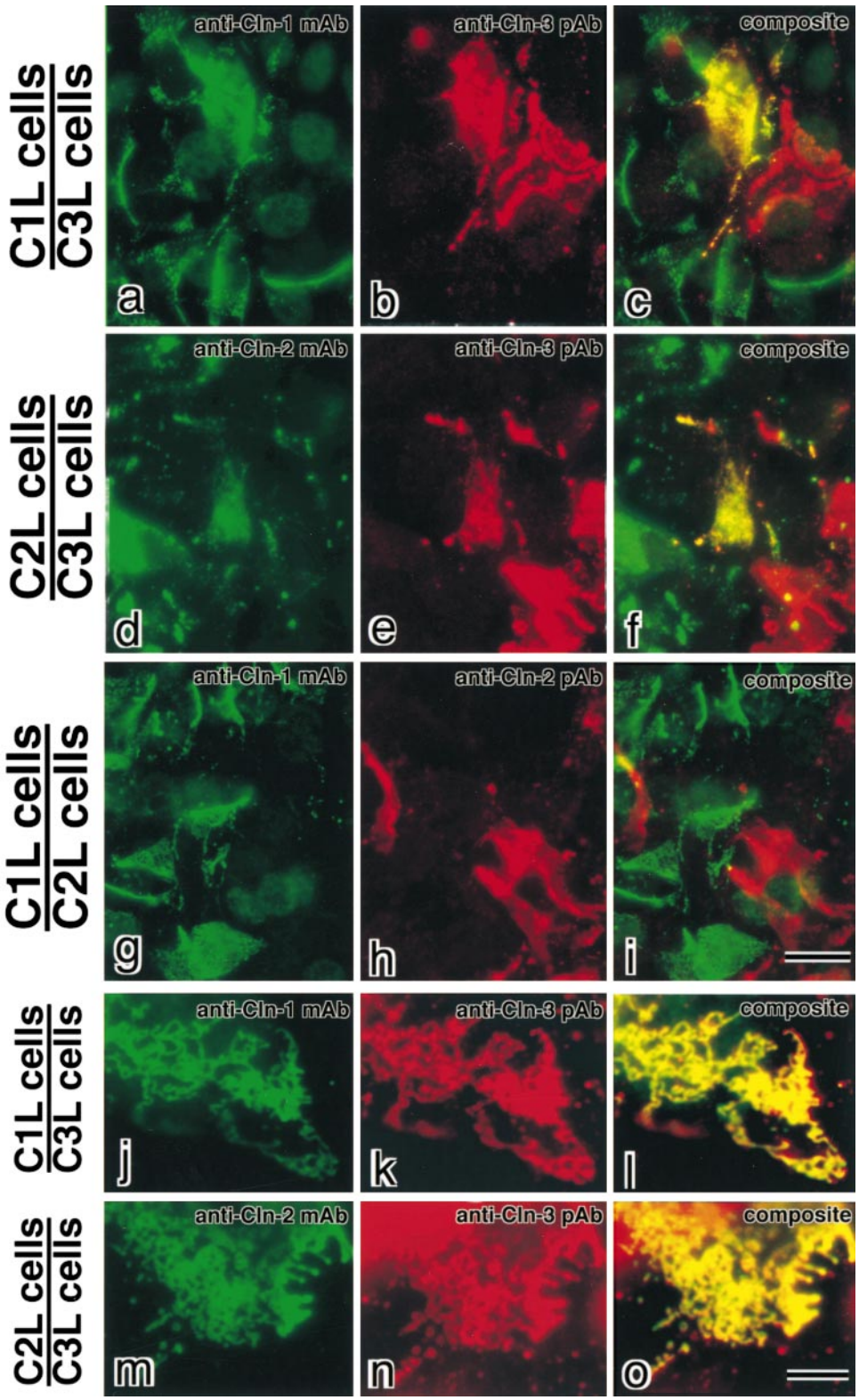

Figure 7. Coculture experiments of two of L transfectants expressing claudin-1 (C1L cells), -2 (C2L cells), or -3 (C3L cells). C1L/C3L (a–c, j–l), C2L/C3L (d–f, m–o), or C1L/C2L (g–i) cocultured cellular sheets were double stained with anticlaudin-1 mAb (green)/anticlaudin-3 pAb (red), anticlaudin-2 mAb (green)/anticlaudin-3 pAb (red), or anticlaudin-1 mAb (green)/anticlaudin-2 pAb (red), respectively. Merged images in the coculture of C1L/C3L (c) and C2L/C3L (f) identified three types of cell–cell contact planes in terms of immunofluorescence staining; green, red, and yellow. Yellow planes were formed between adjacent C1L/C3L cells or C2L/C3L cells. At higher magnification, distinct species of claudins were seen to be recruited to these planes, being precisely coconcentrated in an elaborate network pattern (j–l, m–o). In cocultures of C1L/C2L (i), however, such yellow planes were not observed. We observed 50 fields for C1L/C3L, C2L/C3L, and C1L/C2L coculture experiments and identified yellow planes in 50, 50, and 0 fields, respectively. Bars: (a–i) 10 μm; (j–o) 3 μm.

would be derived from the contact regions between adjacent C2L and C3L cells, were occasionally identified. In these planes, as expected, E-C2L and P-C3L (Fig. 8 c) or E-C3L and P-C2L (data not shown) were seen to be paired. Interestingly, as exemplified in Fig. 8 c, when the fracture plane jumped from the E- to the P-face, the continuity of the network pattern of grooves of E-C2L and strands of P-C3L was completely maintained, conclusively indicating that in these planes individual claudin-2 homopolymers in C2L cells always associated laterally with claudin-3 homopolymers to form TJs in adjacent C3L cells.

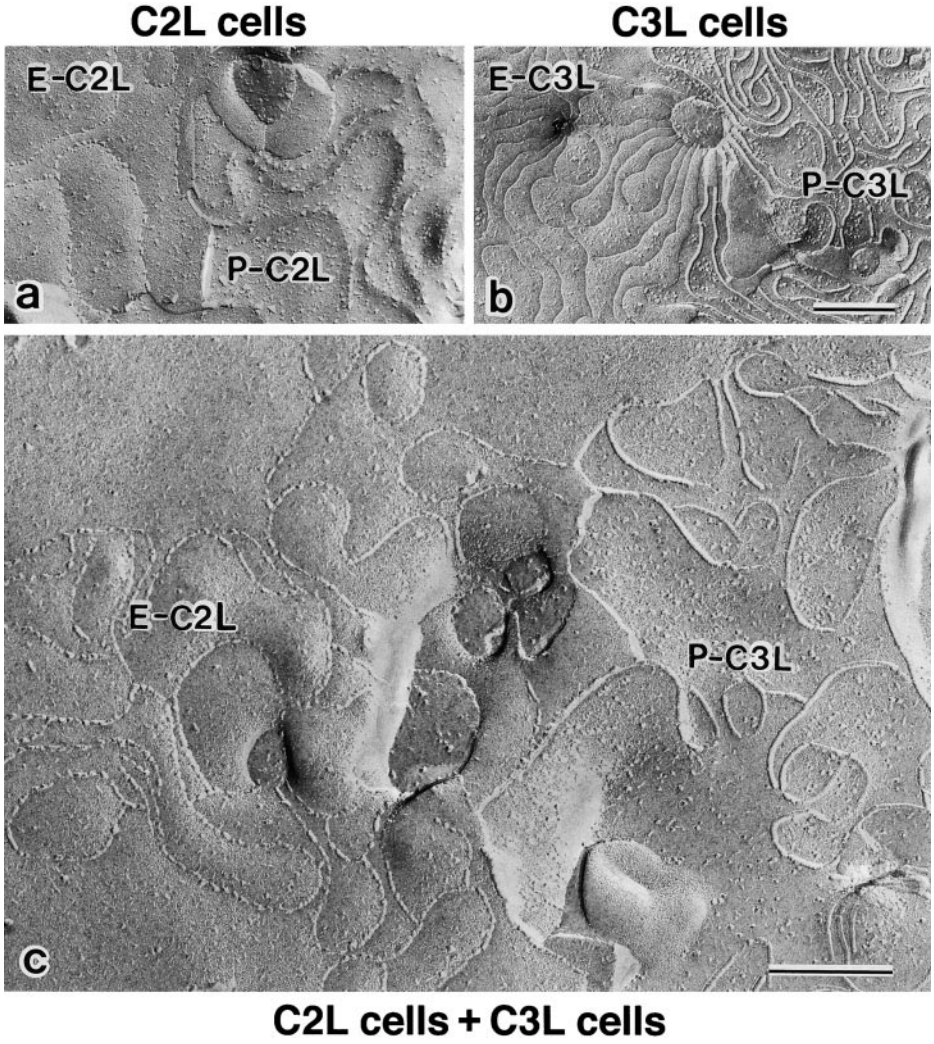

Figure 8. Freeze-fracture replica images of cell–cell contact planes between adjacent C2L and C3L cells. When the cell–cell contact planes in the C2L confluent culture were fractured, the fracture planes were characterized by discontinuous strands on the P-face (P-C2L; a) and grooves occupied with chains of particles on the E-face (E-C2L; a). In contrast, the fracture planes at the contact regions in the C3L confluent culture showed continuous strands on the P-face (P-C3L; b) and vacant grooves on the E-face (E-C3L; b). In the confluent C2L/C3L coculture, in addition to these C2L/C2L and C3L/C3L fracture planes, which would be derived from the contact regions between adjacent C2L and C3L cells, were occasionally identified (c). In these planes, as expected, combinations of E-C2L and P-C3L (c) or E-C3L and P-C2L (data not shown) were observed. When the fracture plane jumped from the E- to the P-face, the continuity of network pattern of grooves of E-C2L and strands of P-C3L were seen to be completely maintained, indicating that in these planes individual claudin-2 homopolymers in C2L cells always associated laterally with claudin-3 homopolymers in adjacent C3L cells. Bars: (a and b) 200 nm; (c) 200 nm.

TJ Strand Formation by Polymerization of Claudin-1 Lacking Its COOH-terminal Cytoplasmic Domain

In this study, we discussed the formation of TJ strands from the viewpoint of claudin–claudin interaction. However, we should consider the possible involvement of peripheral membrane proteins in TJ strand formation. Since the COOH-terminal cytoplasmic domain of claudins was thought to be responsible for their interactions with peripheral membrane proteins, we constructed a claudin-1 mutant lacking its COOH-terminal cytoplasmic domain (claudin-1ΔC), and obtained L transfectants expressing FLAG-tagged claudin-1ΔC (C1ΔCFL cells; Fig. 9 A). These claudin mutants were concentrated at cell–cell borders as shown immunofluorescently in Fig. 9 B. Freeze-fracture replicas obtained from C1ΔCFL cells revealed that this claudin-1 mutant still bore well-developed network of rTJ strands (Fig. 9 C), and interestingly, these rTJ strands were largely associated with the P-face as mostly continuous structures with vacant grooves at the E-face. These findings suggested that the interaction between claudins and peripheral membrane proteins was not required for the formation of TJ strands, per se, as well as their P-face association.

Discussion

Previous studies indicated that claudins are polymerized within plasma membranes to constitute the backbone of TJ strands (Furuse et al., 1998a,b). Furthermore, it is accepted that each TJ strand laterally associates with another TJ strand in apposing membranes to form paired strands. Therefore, there would be two methods of interaction between claudins; the side-by-side interaction for polymerization to form TJ strands, and the head-to-head interaction between each of the paired strands for cell adhesion. Since claudins comprise a multigene family (Furuse et al., 1998a; Morita et al., 1999a; Tsukita and Furuse, 1999), each of the above methods of interaction can be further subdivided into homo- and heterophilic interactions (Fig. 1 B). Therefore, the possible molecular organizations of paired TJ strands can be subclassified into four models (Fig. 1 B, Model A to D). In this study, we evaluated these models using L transfectants expressing claudin-1, -2, and -3 singly or in combination. First, a single species of claudins was sufficient to reconstitute TJ strands, indicating that homopolymers were formed in these cells (see Fig. 2; Furuse et al., 1998b). Furthermore, these homopolymers were associated laterally, both in a homophilic (see Fig. 2),

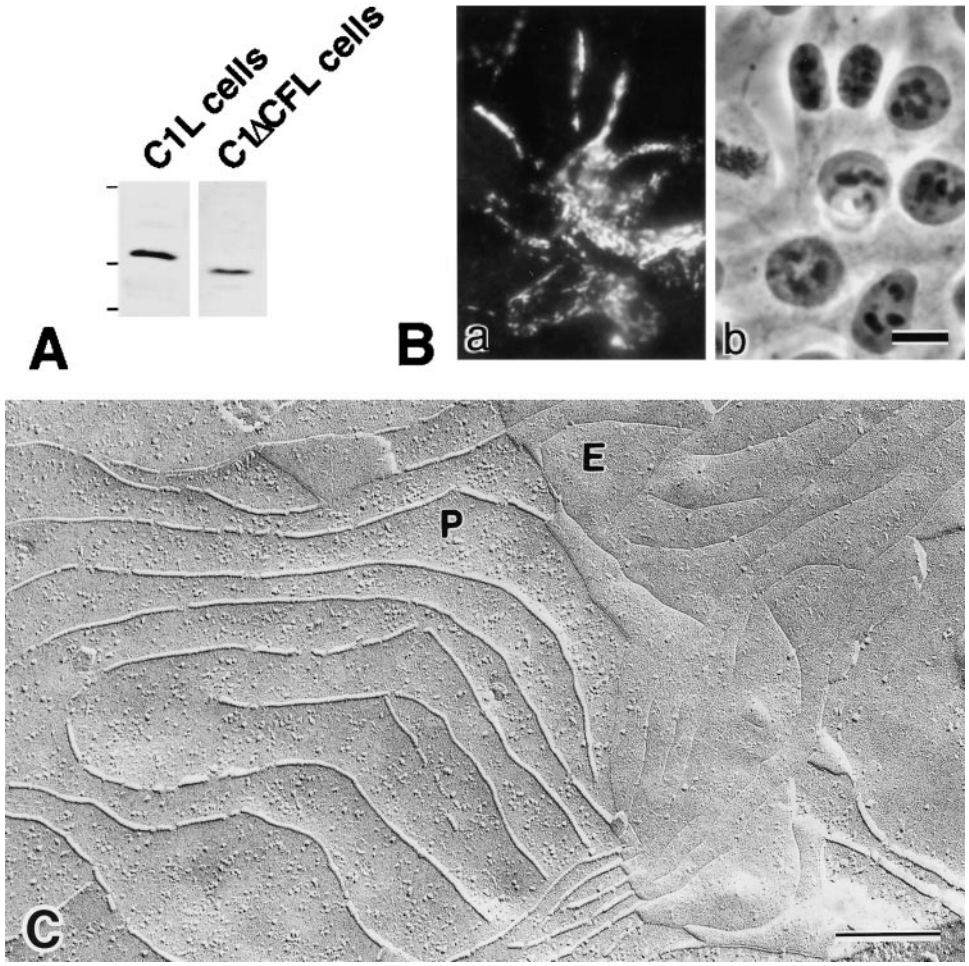

Figure 9. Formation of rTJ strands from claudin-1 mutant lacking its COOH-terminal domain in L cells. A, Total cell lysates of L transfectants expressing claudin-1 (C1L cells) or FLAG-tagged claudin-1 mutant lacking its COOH-terminal domain (C1ΔCFL cells) were immunoblotted with anticlaudin-1 pAb and anti-FLAG mAb, respectively. Bars indicate molecular masses of 31, 21, and 14 kD, respectively, from the top. B, Semiconfluent cultures of C1ΔCFL cells were stained with anti-FLAG mAb (a). Expressed claudin-1 mutant was highly concentrated at cell–cell borders as planes. b, Phase-contrast image. C, Freeze-fracture replica images of induced rTJ strands in C1ΔCFL cells. FLAG-tagged claudin-1 mutant lacking its COOH-terminal domain can form a well-developed network of rTJ strands on the P-face (P) in L cells. E, E-face. Bars: (B) 10 μm; (C) 200 nm.

as well as heterophilic manner (see Fig. 7). Therefore, TJs in L transfectants can adopt both organizations represented in Model A and B (Fig. 1 B). On the other hand, heteropolymers were also induced in L transfectants (see Fig. 4). Models C and D (Fig. 1 B) were not distinguished in the L transfectant system, but since both Model A and B were possible, both Model C and D would also be possible (Fig. 1 B).

The thickness of TJ strands is ~10-nm in freeze-fracture replica images (Staehelin, 1973, 1974). Interestingly, the gap junction channel consisting of six connexins is also ~10-nm in diameter (Kumar and Gilula, 1996; Jiang and Goodenough, 1996). Since connexin also has four transmembrane domains with the same membrane topology as claudins, it is tempting to speculate that oligomers of claudins are also unit structures in TJs, and that these unit structures are arranged linearly to form individual TJ strands. This raises a new question as to whether these unit structures themselves are homomeric or heteromeric, further subdividing the above four models; heteropolymers can be formed by linearly aligned heteromeric unit structures, as well as distinct homomeric unit structures. This type of discussion has been reported in detail for gap junctions, in which the unit structures have been determined (Kumar and Gilula, 1996; Jiang and Goodenough, 1996), but in TJ strands the clarification of unit structures is a prerequisite for further discussion.

Northern blotting showed that most tissues expressed more than two species of claudins (Furuse et al., 1998a; Morita et al., 1999a). Immunofluorescence microscopy revealed that TJs in situ contained claudin-4 and -8 in the kidney (Morita et al., 1999a) and claudin-1, -2, and -3 in the liver (Fig. 3). Therefore, taking the results obtained from the cotransfection experiments (see Figs. 5 and 6), it is likely that in situ most TJ strands are heteropolymers of claudins, although specialized TJ strands in myelin sheaths of oligodendrocytes and in Sertoli cells in the testis appeared to be mainly composed of a single species of claudin, claudin-11 (Morita et al., 1999b). As shown in this study, not only homophilic, but also heterophilic interactions of claudins between each of the paired TJ strands are allowed. Thus, in the paired TJ strands of heteropolymers in situ homophilic interactions of various claudin species, as well as heterophilic interactions between various combinations of claudin species, are expected to occur, as shown in Model D (Fig. 1 B). It is reasonable to postulate that the strength of these interactions varies depending on the claudin species involved and their combinations, and that the tightness of each TJ strand is determined as a whole by the number/type of species of claudins and their mixing ratio in the strand. For example, MDCK I cells have a fairly tighter TJ barrier than MDCK II cells, but no difference was detected in the number of TJ strands between these two distinct clones of MDCK cells (Stevenson

et al., 1988). These observations suggested a qualitative difference of the paired TJ strands in their tightness between these two clones, and this difference could be explained as postulated above.

To avoid further complexity, we have not discussed occludin. Immunoreplica analyses indicated that occludin was also incorporated into TJ strands in situ in most types of epithelial cells (Fujimoto, 1995; Furuse et al., 1996; Saitou et al., 1997). When occludin was cotransfected into L cells, together with claudin-1, they were coincorporated into rTJ strands (and of course also paired rTJ strands; Furuse et al., 1998b). Occludin singly introduced into L cells was concentrated at cell–cell borders in a punctate manner, indicating that occludins interact with each other in a homophilic manner between adjacent cells (Furuse et al., 1998b). Furthermore, when L transfectants expressing occludin were cocultured with C1L cells, neither occludin or claudin-1 was concentrated at cell–cell borders, suggesting that occludin does not interact with claudin-1 in a heterophilic manner between adjacent cells (Furuse, M., and S. Tsukita, unpublished data). Therefore, at present it is very difficult to postulate how occludin is incorporated into the paired heteropolymers of claudins (TJ strands) in situ. Occludin may be incorporated into claudin-based TJ strands in the same manner as claudins, and in the paired TJ strands occludin may be positioned opposite to occludin, which allows occludin–occludin interaction (Furuse et al., 1998b). Alternatively, it may be positioned opposite to a claudin which may result in the formation of small pores. It is also possible that occludin is involved in TJ strand formation differently from claudins.

Finally, we should discuss the possible role of peripheral membrane proteins, such as ZO-1 (Stevenson et al., 1986), ZO-2 (Gumbiner et al., 1991), and ZO-3 (Balda et al., 1993; Haskins et al., 1998) in the formation of TJ strands. ZO-1, but not ZO-2 or ZO-3, was expressed endogenously in L cells, and this endogenous ZO-1 was coconcentrated with claudin-1 and -2 at cell–cell borders as an elaborate network in C1L and C2L cells, respectively (Itoh, M., M. Furuse, K. Morita, and S. Tsukita, unpublished data). In our previous study (Furuse et al., 1998b), we reported that claudin-1 and -2 with a FLAG tag at their COOH-termini also formed a well-developed network of rTJ strands in L transfectants. Interestingly, however, endogenous ZO-1 was not recruited to these FLAG-claudin-1 or FLAG-claudin-2–based rTJ strands, probably because the FLAG sequence affected the claudin/ZO-1 interaction (Furuse, M., and S. Tsukita, unpublished data). These findings indicated that ZO-1 (and also ZO-2 and ZO-3) was not required for the formation of rTJ strands in L transfectants. Furthermore, Fig. 9 showed that a claudin-1 deletion mutant lacking almost all of its COOH-terminal cytoplasmic domain still formed a well-developed network of rTJ strands in L transfectants, favoring the notion that the peripheral membrane proteins are not involved in the polymerization of claudins within plasma membranes. Therefore, we interpreted the data presented in this study without considering the possible involvement of peripheral membrane proteins.

The model system of L transfectants used in this study was very useful to analyze the properties of each claudin species. To date, 15 members of the claudin family have been identified, but it remains unclear how many claudins will be identified in the future. It is thus very difficult, by the use of epithelial cells, to clarify the nature and function of each claudin species, partly because we cannot determine exactly all the types of claudins expressed in certain epithelial cells. Therefore, to further understand the structure and functions of claudins and TJ strands, the L transfectant system will continue to be used towards the reconstitution of TJs as a complementary technique to the knockout of each claudin gene.

We thank all the members of our laboratory (Department of Cell Biology, Faculty of Medicine, Kyoto University) for helpful discussions. Our thanks are also due to Ms. K. Yoshida, K. Fukui, and Ms. K. Furuse for their excellent technical assistance, and to Drs. K. Morita and N. Sonoda (Kyoto University) for construction of the claudin-3 expression vector and production of mAbs, respectively.

This study was supported in part by a grant-in-aid for Cancer Research and a grant-in-aid for Scientific Research (A) from the Ministry of Education, Science, and Culture of Japan to S. Tsukita and in part by a grant from the Kazato Research Foundation to M. Furuse.

Submitted: 15 June 1999
Revised: 28 September 1999
Accepted: 30 September 1999

Note Added in Proof. Positional cloning has identified a new member of the claudin family (paracellin-1/claudin-16) in which mutations cause hereditary renal hypomagnesemia in humans (Simon, D.B., Y. Lu, K.A. Choate, H. Velazquez, E. Al-Sabban, M. Praga, G. Casari, A. Bettinelli, G. Colussi, J. Rodriguez-Soriano, et al. 1999. Paracellin-1, a renal tight junction protein required for paracellular Mg^{2+} resorption. *Science.* 285: 103–106). This finding favors the idea that claudins possibly are involved in the formation of aqueous pores within TJ strands.

References

Anderson, J.M., and C.M. van Itallie. 1995. Tight junctions and the molecular basis for regulation of paracellular permeability. *Am. J. Physiol.* 269:G467–G475.

Ando-Akatsuka, Y., M. Saitou, T. Hirase, M. Kishi, A. Sakakibara, M. Itoh, S. Yonemura, M. Furuse, and Sh. Tsukita. 1996. Interspecies diversity of the occludin sequence: cDNA cloning of human, mouse, dog, and rat-kangaroo homologues. *J. Cell Biol.* 133:43–47.

Balda, M.S., L. González-Mariscal, K. Matter, M. Cereijido, and J.M. Anderson. 1993. Assembly of the tight junction: the role of diacylglycerol. *J. Cell Biol.* 123:293–302.

Balda, M.S., J.A. Whitney, C. Flores, S. González, M. Cereijido, and K. Matter. 1996. Functional dissociation of paracellular permeability and transepithelial electrical resistance and disruption of the apical–basolateral intramembrane diffusion barrier by expression of a mutant tight junction membrane protein. *J. Cell Biol.* 134:1031–1049.

Chen, Y.-H., C. Merzdorf, D.L. Paul, and D.A. Goodenough. 1997. COOH terminus of occludin is required for tight junction barrier function in early *Xenopus* embryos. *J. Cell Biol.* 138:891–899.

Claude, P. 1978. Morphological factors influencing transepithelial permeability: a model for the resistance of the zonula occludens. *J. Membr. Biol.* 10:219–232.

Farquhar, M.G., and G.E. Palade. 1963. Junctional complexes in various epithelia. *J. Cell Biol.* 17:375–412.

Fujimoto, K. 1995. Freeze-fracture replica electron microscopy combined with SDS digestion for cytochemical labeling of integral membrane proteins. Application to the immunogold labeling of intercellular junctional complexes. *J. Cell Sci.* 108:3443–3449.

Furuse, M., T. Hirase, M. Itoh, A. Nagafuchi, S. Yonemura, Sa. Tsukita, and Sh. Tsukita. 1993. Occludin: a novel integral membrane protein localizing at tight junctions. *J. Cell Biol.* 123:1777–1788.

Furuse, M., K. Fujimoto, N. Sato, T. Hirase, Sa. Tsukita, and Sh. Tsukita. 1996. Overexpression of occludin, a tight junction-associated integral membrane protein, induces the formation of intracellular multilamellar bodies bearing tight junction-like structures. *J. Cell Sci.* 109:429–435.

Furuse, M., K. Fujita, T. Hiiragi, K. Fujimoto, and Sh. Tsukita. 1998a. Claudin-1 and -2: novel integral membrane proteins localizing at tight junctions with no sequence similarity to occludin. *J. Cell Biol.* 141:1539–1550.

Furuse, M., H. Sasaki, K. Fujimoto, and Sh. Tsukita. 1998b. A single gene product, claudin-1 or -2, reconstitutes tight junction strands and recruits occludin in fibroblasts. *J. Cell Biol.* 143:391–401.

Gumbiner, B. 1993. Breaking through the tight junction barrier. *J. Cell Biol.*

123:1631–1633.

Gumbiner, B., T. Lowenkopf, and D. Apatira. 1991. Identification of a 160 kDa polypeptide that binds to the tight junction protein ZO-1. *Proc. Natl. Acad. Sci. USA*. 88:3460–3464.

Haskins, J., L. Gu, E.S. Wittchen, J. Hibbard, and B.R. Stevenson. 1998. ZO-3, a novel member of the MAGUK protein family found at the tight junction, interacts with ZO-1 and occludin. *J. Cell Biol.* 141:199–208.

Hirase, T., J.M. Staddon, M. Saitou, Y. Ando-Akatsuka, M. Itoh, M. Furuse, K. Fujimoto, Sh. Tsukita, and L.L. Rubin. 1997. Occludin as a possible determinant of tight junction permeability in endothelial cells. *J. Cell Sci.* 110:1603–1613.

Itoh, M., S. Yonemura, A. Nagafuchi, Sa. Tsukita, and Sh. Tsukita. 1991. A 220-kD undercoat-constitutive protein: its specific localization at cadherin-based cell–cell adhesion sites. *J. Cell Biol.* 115:1449–1462.

Jiang, J.X., and D.A. Goodenough. 1996. Heteromeric connexons in lens gap junction channels. *Proc. Natl. Acad. Sci. USA*. 93:1287–1291.

Kubota, K., M. Furuse, H. Sasaki, N. Sonoda, K. Fujita, A. Nagafuchi, and Sh. Tsukita. 1999. Ca^{++}-independent cell adhesion activity of claudins, integral membrane proteins of tight junctions. *Curr. Biol.* 9:1035–1038.

Kumar, N.M., and N.B. Gilula. 1996. The gap junction communication channel. *Cell.* 84:381–388.

Laemmli, U.K. 1970. Cleavage of structural proteins during the assembly of the head of bacteriophage T4. *Nature.* 227:680–685.

Martin-Padura, I., S. Lostaglio, M. Schneemann, L. Williams, M. Romano, P. Fruscella, C. Panzeri, A. Stoppacciaro, L. Ruco, A. Villa, et al. 1998. Junctional adhesion molecule, a novel member of the immunoglobulin superfamily that distributes at intercellular junctions and modulates monocyte transmigration. *J. Cell Biol.* 142:117–127.

McCarthy, K.M., I.B. Skare, M.C. Stankewich, M. Furuse, S. Tsukita, R.A. Rogers, R.D. Lynch, and E.E. Schneeberger. 1996. Occludin is a functional component of the tight junction. *J. Cell Sci.* 109:2287–2298.

Moroi, S., M. Saitou, K. Fujimoto, A. Sakakibara, M. Furuse, O. Yoshida, and Sh. Tsukita. 1998. Occludin is concentrated at tight junctions of mouse/rat but not human/guinea pig Sertoli cells in testes. *Am. J. Physiol.* 274:C1708–C1717.

Morita, K., M. Furuse, K. Fujimoto, and Sh. Tsukita. 1999a. Claudin multigene family encoding four-transmembrane domain protein components of tight junction strands. *Proc. Natl. Acad. Sci. USA*. 96:511–516.

Morita, K., H. Sasaki, K. Fujimoto, M. Furuse, and Sh. Tsukita. 1999b. Claudin-11/OSP-based tight junctions in myelinated sheaths of oligodendrocytes and Sertoli cells in testis. *J. Cell Biol.* 145:579–588.

Niwa, H., K. Yamamura, and J. Miyazaki. 1991. Efficient selection for high-expression transfectants with a novel eukaryotic vector. *Gene.* 108:193–200.

Powell, D.W. 1981. Barrier function of epithelia. *Am. J. Physiol.* 241:G275–G288.

Saitou, M., Y. Ando-Akatsuka, M. Itoh, M. Furuse, J. Inazawa, K. Fujimoto, and Sh. Tsukita. 1997. Mammalian occludin in epithelial cells: its expression and subcellular distribution. *Eur. J. Cell Biol.* 73:222–231.

Saitou, M., K. Fujimoto, Y. Doi, M. Itoh, T. Fujimoto, M. Furuse, H. Takano, T. Noda, and Sh. Tsukita. 1998. Occludin-deficient embryonic stem cells can differentiate into polarized epithelial cells bearing tight junctions. *J. Cell Biol.* 141:397–408.

Santerre, R.F., N.E. Allen, J.N. Hobbs, Jr., R.N. Rao, and R.J. Schmidt. 1984. Expression of prokaryotic genes for hygromycin B and G418 resistance as dominant-selection markers in mouse L cells. *Gene.* 30:147–156.

Schneeberger, E.E., and R.D. Lynch. 1992. Structure, function, and regulation of cellular tight junctions. *Am. J. Physiol.* 262:L647–L661.

Staehelin, L.A. 1973. Further observations on the fine structure of freeze-cleaved tight junctions. *J. Cell Sci.* 13:763–786.

Staehelin, L.A. 1974. Structure and function of intercellular junctions. *Int. Rev. Cytol.* 39:191–283.

Stevenson, B.R., J.M. Anderson, D.A. Goodenough, and M.S. Mooseker. 1988. Tight junction structure and ZO-1 content are identical in two strains of Madin-Darby canine kidney cells which differ in transepithelial resistance. *J. Cell Biol.* 107:2401–2408.

Stevenson, B.R., J.D. Siliciano, M.S. Mooseker, and D.A. Goodenough. 1986. Identification of ZO-1: a high molecular weight polypeptide associated with the tight junction (zonula occludens) in a variety of epithelia. *J. Cell Biol.* 103:755–766.

Tsukita, Sh., and M. Furuse. 1999. Occludin and claudins in tight junction strands: leading or supporting players? *Trends Cell Biol.* 9:268–273.

Wong, V., and B.M. Gumbiner. 1997. A synthetic peptide corresponding to the extracellular domain of occludin perturbs the tight junction permeability barrier. *J. Cell Biol.* 136:399–409.

Yap, A.S., J.M. Mullin, and B.R. Stevenson. 1998. Molecular analysis of tight junction physiology: insights and paradoxes. *J. Membr. Biol.* 163:159–167.